Magnetic-field switching of second-harmonic generation in noncentrosymmetric magnet $Eu_2MnSi_2O_7$

Shingo Toyoda,[1,*] Jiou-Cing Liao,[2] Guang-Yu Guo,[2,3] Yusuke Tokunaga,[4] Taka-hisa Arima,[1,4] Yoshinori Tokura,[1,5,6] and Naoki Ogawa[1,5]

[1]*RIKEN Center for Emergent Matter Science (CEMS), Saitama 351-0198, Japan*
[2]*Department of Physics, National Taiwan University, Taipei 10617, Taiwan*
[3]*Physics Division, National Center for Theoretical Sciences, Taipei 10617, Taiwan*
[4]*Department of Advanced Materials Science, University of Tokyo, Kashiwa 277-8561, Japan*
[5]*Department of Applied Physics, The University of Tokyo, Tokyo 113-8656, Japan*
[6]*Tokyo College, University of Tokyo, Tokyo 113-8656, Japan*

(Received 9 December 2022; accepted 26 January 2023; published 9 February 2023)

We report a giant magnetic-field effect on optical second-harmonic generation (SHG) in a noncentrosymmetric ferrimagnet $Eu_2MnSi_2O_7$. The SHG intensity changes at visible photon energy of 2.8 eV by more than 7000% upon the reversal of magnetic-field direction. Such pronounced modulation of the nonlinear optical activity results from an interference between crystallographic and magnetically induced nonlinear polarization. The amplitude of these nonlinear optical susceptibilities is controlled by the spin alignment and the light incident angle, enabling to optimize the magnetic switching of SHG in detail.

DOI: 10.1103/PhysRevMaterials.7.024403

I. INTRODUCTION

Symmetry plays an essential role in the physical response of a material. In optical responses, for example, the time-reversal symmetry breaking leads to magneto-optical Kerr and Faraday effects, whereas the breaking of the spatial-inversion symmetry gives rise to the second-order nonlinear optical effects as exemplified by second-harmonic generation (SHG) which is a frequency-doubling process of a light wave. The SHG is generally insensitive to the magnetization or magnetic field because axial vectors will not couple to the spatial-inversion symmetry. When time-reversal and spatial-inversion symmetries are simultaneously broken, however, unique magneto-optical effects, such as nonreciprocal directional dichroism [1–8] and magnetization-induced SHG (MSHG) [9–20] can show up. In the spin-lattice system with reduced symmetry by a magnetic order, an additional contribution to nonlinear polarization $P_i(2\omega)$ appears, which is given by

$$P_i(2\omega) = \epsilon_0\left(\chi^{\mathrm{cry}}_{ijk} + \chi^{\mathrm{mag}}_{ijkl}M_l\right)E_j(\omega)E_k(\omega),$$

where $E(\omega)$ is the electric field of the incident light and M_l the spontaneous magnetization [16]. Here $\chi^{\mathrm{cry}}_{ijk}$ and $\chi^{\mathrm{mag}}_{ijkl}$ denote the crystallographic SHG and magnetically induced SHG (MSHG) susceptibilities, respectively; the former is a rank-3 polar tensor which originates from the noncentrosymmetric crystal (lattice) structure, whereas the latter is a rank-4 axial tensor which appears only below the magnetic ordering temperature or in a magnetic field. The interference between these two contributions results in a change in the SHG intensity $I(2\omega) \propto P^2(2\omega) \propto (\chi^{\mathrm{cry}}_{ijk} + \chi^{\mathrm{mag}}_{ijkl}M_l)^2$ with the reversal of M_l as depicted in Fig. 1. Especially, when a crystallographic term has amplitude and phase comparable to those of the corresponding MSHG term, $I(2\omega)$ is enhanced in a positive field owing to the constructive interference, whereas the destructive interference extinguishes its intensity in a negative magnetic field [20]. However, the realization of such a condition is a challenge owing to the fact that the nonlinear polarization from $\chi^{\mathrm{cry}}_{ijk}$ and $\chi^{\mathrm{mag}}_{ijkl}$ contributions normally have 90° phase shift between each other because $\chi^{\mathrm{cry}}_{ijk}$ is a real tensor, whereas, $\chi^{\mathrm{mag}}_{ijkl}$ is an imaginary one in a photon-energy range without optical absorption [15,16,20], and, thus, the interference does not occur. Precise tuning of complex $\chi^{\mathrm{cry}}_{ijk}$ and $\chi^{\mathrm{mag}}_{ijkl}$ (in both amplitude and phase) is, in fact, necessary to realize perfect interference.

Here, we report on the magnetic control of the SHG in noncentrosymmetric ferrimagnet $Eu_2MnSi_2O_7$ by achieving the above condition. We have successfully grown single crystals of $Eu_2MnSi_2O_7$ and found that a MSHG signal which scales with M^2 appears below the Curie temperature T_C = 10.7 K. The interference between the crystallographic SHG and the MSHG occurs with nearly the same magnitude and phase, which realizes a large magnetic modulation of the SHG signal up to 7000% at a visible photon energy with the reversal of a magnetic field. Our first-principles calculation has revealed that $\chi^{\mathrm{cry}}_{ijk}$ and $\chi^{\mathrm{mag}}_{ijkl}$ have almost same phases at a photon energy around 2.8 eV where the effect is the most pronounced, enabling to realize the large magnetic contrast of the SHG signal.

The melilite-type oxide compounds $A_2MM'_2O_7$ (A: larger divalent alkali earth or lanthanide ions, M, M': smaller di-, tri-, or tetravalent ions) show intriguing phenomena, such as magneto-electric coupling [21–23] and optical nonreciprocity

*Present address: Department of Physics, University of California, Berkeley, California 94720, USA; toyoda@berkeley.edu

 ©2023 American Physical Society

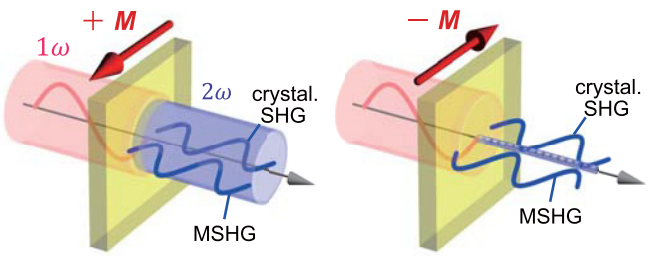

FIG. 1. Schematic of experimental setup to detect the magnetically controllable SHG. The SHG intensity largely changes with the reversal of magnetization direction. The crystallographic SHG contribution is unaffected by the magnetization direction, whereas the MSHG signal changes sign upon the time-reversal operation. They constructively (left) or destructively (right) interfere with each other for the positive and negative magnetization direction, respectively, producing the large contrast in the SHG intensity.

[7,8] due to the simultaneous breaking of the time-reversal and spatial-inversion symmetries. In the past, a wide variety of magnetic properties has been found including spin-glass [24], antiferromagnetic [21], ferrimagnetic [25], and spin-spiral [26] magnetic behaviors. Among them, ferrimagnetic $Eu_2MnSi_2O_7$ with large magnetization (9 μ_B / f.u.) is ideal to investigate MSHG because its susceptibility is expected to be proportional to magnetization M.

II. EXPERIMENTAL DETAILS

Single crystals of $Eu_2MnSi_2O_7$ were grown by the floating-zone method. The polycrystalline feed and seed rods for the crystal growth were prepared by the solid-state reaction. First, the stoichiometric mixture of powders of Eu_2O_3, MnO, SiO_2, and Si were calcined at 1050 °C for 12 h in the flow of Ar. Then, the resultant product was pressed into rods and sintered at 1100 °C for 24 h in the same gas condition. The crystal growth was carried out in the atmospheres of 5–10 atm Ar. The obtained crystals showed yellowish color. They were oriented using Laue x-ray photography and cut into thin plates of thickness 130 μm. Two platelets were used for measurements: One had the widest faces perpendicular to the crystallographic [010] axis, and the other had the faces tilted by 16° around the [100] axis from the (010) plane as shown in Fig. 3(a). The interference between the crystallographic SHG and MSHG with normal incidence was predicted to occur only for the latter sample because of the selection rule (see the detailed discussion below). The samples were specularly polished by alumina lapping films, characterized by a superconducting quantum interference device magnetometer and mounted on a copper holder in a superconducting magneto-optical cryostat. The wavelength of the incident laser pulses (160 fs at 6-kHz repetition rate) was controlled by an optical parametric amplifier. The SHG intensity at normal incidence was detected in a transmission geometry by a liquid-nitrogen-cooled charge-coupled device camera.

$Eu_2MnSi_2O_7$ crystallizes in a noncentrosymmetric tetragonal structure with the space-group $P\bar{4}2_1m$ (point-group $\bar{4}2m$) [25]. The crystal is characterized by alternating stacking of manganese and europium layers along the c axis. The Mn^{2+} and Si^{4+} ions occupy tetrahedral sites coordinated by four oxygen ions [Fig. 2(a)]. MnO_4 and SiO_4 tetrahedra share an oxygen ion at a corner and form layers on the ab plane. The Eu^{2+} ions occupy a highly distorted site surrounded by eight oxygen ions and intervene between two Mn layers. The magnetic ions Eu^{2+} ($4f^7$, 7 μ_B) and Mn^{2+} ($3d^5$, 5-μ_B) show ferrimagnetic ordering below $T_C = 10.7$ K [25]. The saturation magnetization value ∼9 μ_B/f.u. suggests that, whereas the magnetic interaction within the layer is ferromagnetic, the manganese layer (5 μ_B/f.u.) is antiferromagnetically coupled with the adjacent europium layer (14 μ_B/f.u.). However, detailed magnetic properties of $Eu_2MnSi_2O_7$ remain elusive because a polycrystalline sample was used in previous research [25].

III. RESULTS AND DISCUSSION

We show in Fig. 2(b) the temperature dependence of magnetization in a magnetic field of 0.1 T applied in the [001] and [100] directions. Our measurement using a single crystal reveals an easy-plane type magnetic anisotropy with the [001] axis being the magnetic hard axis. Figure 2(c) shows the magnetic-field dependence of magnetization at 2 K. The magnetic moments can be easily aligned with a weak magnetic field of ∼50 mT in the basal plane, whereas the anisotropy

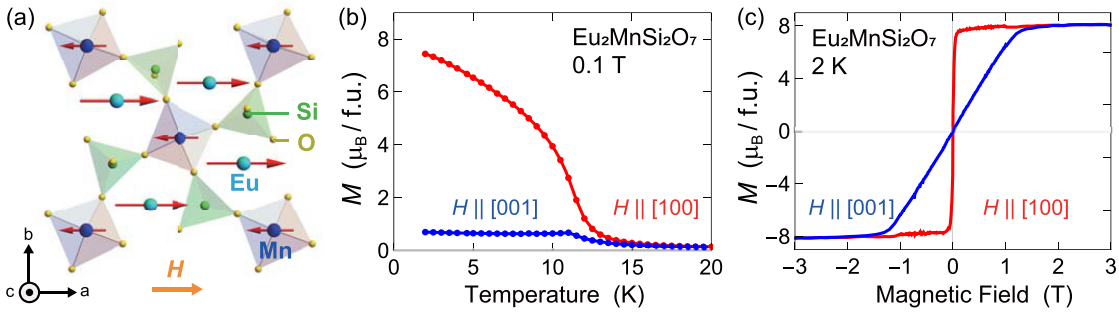

FIG. 2. (a) Crystal structure of $Eu_2MnSi_2O_7$ projected onto the (001) plane together with the magnetic structure in the ferrimagnetic phase below T_C. Red arrows show magnetic moments of Eu^{2+} (7 μ_B) and Mn^{2+} (5 μ_B) ions in the ferrimagnetic phase in a magnetic-field H||[100] where the lengths of the arrows schematically represent the size of the moments. (b) Temperature dependence of magnetization in a DC magnetic field of $\mu_0 H = 0.1$ T in the [100] and [001] directions, measured in the field-cooling process. (c) Magnetization curve at $T = 2$ K for the magnetic field along the [100] and [001] axes.

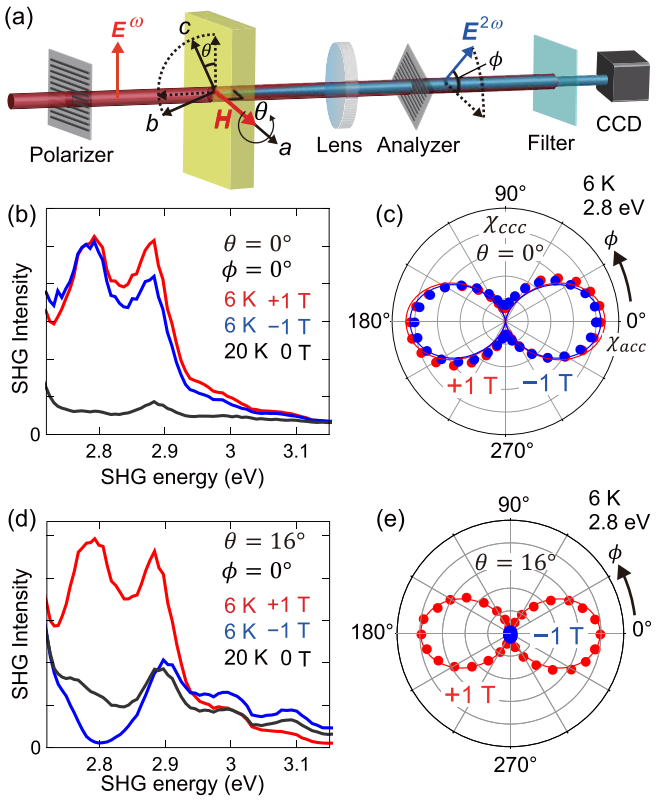

FIG. 3. (a) Schematic of the experimental setup. SHG is measured in a transmission geometry for two platelets of single crystals: One has the (010) surface as the widest faces, and the other is tilted by an angle of $\theta = 16^\circ$ around the a axis. The external magnetic field is applied along the a axis. (b) and (d) SHG spectra with the polarization of $E^{2\omega} \parallel [100]$ measured for $+1$ T (red) and -1 T (blue) at 6 K for (b) (010)-oriented sample and (d) tilted sample by $\theta = 16^\circ$. The black lines show the spectra at 20 K (above Curie temperature) without an external magnetic field. (c) and (e) SHG polarization anisotropy measured by rotating the analyzer in a magnetic field of $+1$ T (red) and -1 T (blue) for (c) (010)-oriented sample and (e) sample tilted by $\theta = 16^\circ$. The solid lines in (c) and (d) are fits corresponding to the tensor components $\chi^{\rm mag}_{acca}$ and $\chi^{\rm cry}_{abc}$.

field is estimated to be ∼1.2 T. The saturation magnetization 8.1 μ_B at 3 T is close to 9 μ_B expected from the simple ferrimagnetic structure [25]. We show in Fig. 2(a) the magnetic structure of $Eu_2MnSi_2O_7$ in a magnetic field along the [100] axis. The magnetic ordering reduces the symmetry of the spin-lattice system from $\bar{4}2m1'$ to $22'2'$ with the a axis being a twofold rotation axis, generating the additional SHG tensor components below T_C. The $\bar{4}2m$ point group allows the crystallographic SHG with the tensor components $\chi^{\rm cry}_{abc}$, $\chi^{\rm cry}_{bca}$, and $\chi^{\rm cry}_{\rm cab}$ above T_C, whereas the MSHG from the tensor components $\chi^{\rm mag}_{aaaa}$, $\chi^{\rm mag}_{abba}$, $\chi^{\rm mag}_{acca}$, $\chi^{\rm mag}_{baba}$, and $\chi^{\rm mag}_{ccaa}$ become allowed in the magnetic point group $22'2'$ with the magnetization along the a axis.

We perform SHG spectroscopy with the experimental setup shown in Fig. 3(a). For the (010)-oriented sample, the crystallographic SHG is forbidden for the normal incidence and only MSHG is allowed because the c component of the electric field of light is absent. Meanwhile, both the contributions are allowed for the tilted sample and may result in some interference between them. We show in Fig. 3(b) SHG spectra taken with the (010)-oriented sample at 6 K. A large SHG signal is observed between 2.7 and 2.9 eV, which can be assigned to MSHG. Figure 3(c) shows the polarization dependence of the SHG signal at a photon energy $2\hbar\omega = 2.8$ eV, which is obtained by rotating the analyzer whereas keeping the polarization of the incident light parallel to the [001] axis. The SHG polarization anisotropy is well fitted by considering the MSHG tensor component $\chi^{\rm mag}_{acca}$, in good agreement with the magnetic point-group $22'2'$. The SHG intensity scales with M^2 (see the Supplemental Material [27]), which confirms that the observed signal is assigned to MSHG.

The crystallographic SHG for $\chi^{\rm cry}_{abc}$ becomes allowed when the sample is tilted around the a axis because the electric field of light contains the c-axis component. Although the crystallographic SHG is unaffected by the time-reversal operation, the MSHG changes its sign as shown in Fig. 1. We show in Fig. 3(d) SHG spectra taken with the sample tilted by $\theta = 16^\circ$ at 6 K. We observe a large change in the SHG signal around 2.8 eV with the reversal of an external magnetic field of 1 T in contrast to the (010)-oriented platelet. The SHG anisotropy in Fig. 3(e) suggests that the SHG intensity

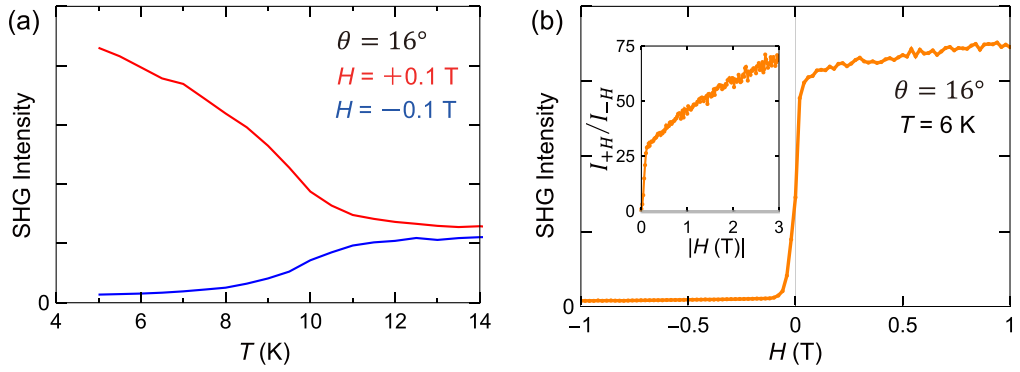

FIG. 4. (a) Temperature dependence of the SHG intensity at 2.8 eV in magnetic fields of ±0.1 T. (b) Magnetic-field dependence of the SHG at 6 K for the photon energy at 2.8 eV. The inset shows the SHG intensity ratio with the reversal of a magnetic field as a function of the magnitude of the magnetic field (see the text).

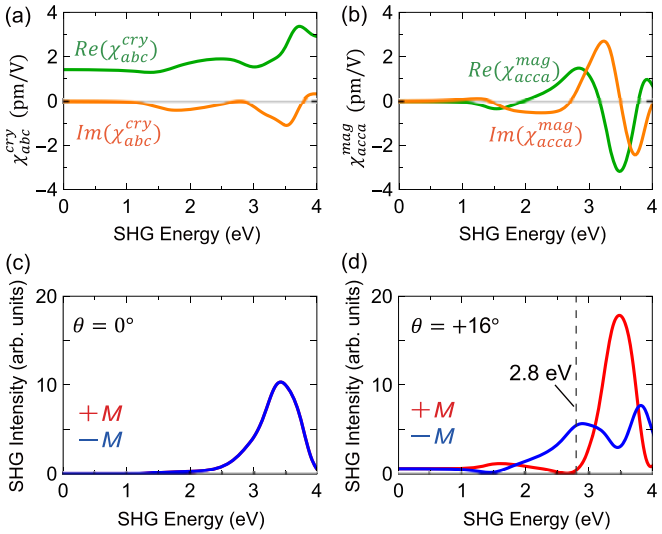

FIG. 5. (a) and (b) Spectra of the SHG susceptibilities from the first-principles calculation. The real and imaginary parts of the susceptibility of (a) the crystallographic SHG for $\chi^{\rm cry}_{abc}$ and (b) the MSHG for $\chi^{\rm mag}_{acca}M_a$ with $M_a = 9\,\mu_{\rm B}$/f.u. (c) and (d) The calculated SHG spectra for (c) (010)-oriented sample and (d) tilted sample by $\theta = 16^\circ$. The red and blue lines are the spectra for the positive and negative saturated magnetization, respectively. For (c), the spectra for $\pm M$ are overlapped with each other.

diminishes for a negative magnetic field, whereas it keeps a large intensity for a positive field. This is in stark contrast to the nonlinear magneto-optical Kerr effect where the SHG polarization rotates with the time-reversal operation [10,17].

Figure 4(a) shows temperature dependence of the SHG at 0.1 T for the tilted platelet. Strikingly, the SHG signal diminishes with lowering temperature below $T_{\rm C}$ for the negative magnetic field, suggesting that a destructive interference occurs with the crystallographic SHG. Figure 4(b) shows magnetic-field dependence of the SHG signal at 6 K. The signal vanishes for the negative field whereas it is enhanced for the positive field, indicating the interference of the MSHG with the crystallographic SHG of the comparable amplitude and phase. The inset of Fig. 4(b) indicates the intensity ratio I_{+H}/I_{-H} with the reversal of a magnetic field as a function of the external magnetic-field strength $|H|$. The SHG intensity ratio increases with the magnetic field to above 7000% at $\mu_0 H = 3$ T.

To further elucidate the origin of the magnetically modulated SHG signal, we calculate nonlinear optical susceptibility by using first-principles calculations (see the Supplemental Material [27] and references [28–38] therein for the calculation details). We show the calculated real and imaginary parts of the SHG susceptibilities of the crystallographic SHG in Fig. 5(a) and of the MSHG in Fig. 5(b). Strikingly, both the crystallographic SHG and MSHG have a large susceptibility for the real part at 2.8 eV, whereas the imaginary part is negligibly small. Hence, these two contributions can interfere with each other in the same phase. Figure 5(c) shows the calculated SHG spectrum for the (010)-oriented sample. The signal is unchanged with the time-reversal operation because the SHG is solely from the MSHG. On the other hand, when the sample is tilted by $\theta = 16^\circ$, the SHG signal around 2.7 eV shows a large change with the reversal of a magnetic field as shown in Fig. 5(d). This is in excellent agreement with the experimentally observed results except a slight shift in the photon energy. Although the calculated SHG intensity increases with the photon energy, the experimentally observed SHG spectrum shows more complicated photon-energy dependence. The deviation in the spectrum shape between the calculation and experiment can be ascribed to large optical absorption due to the $4f$-$5d$ transition of Eu ions and resultant modification of the phase-matching condition with the photon energy, which significantly affects the SHG intensity.

A similar magnetic switching of SHG is observed in CuB_2O_4 where the magnetic contrast results from an interference of the crystallographic SHG of electric dipole origin and magnetic dipole MSHG [18]. Since the electric (magnetic) dipole transition is even (odd) function of the wave vector of light $\vec{k}$, the SHG is nonreciprocal in CuB_2O_4, i.e., its intensity changes upon the reversal of the propagation direction of light. In the present paper, the SHG intensity remains unchanged upon the reversal of $\vec{k}$ because both the crystallographic SHG and the MSHG originate from the electric dipole transitions.

IV. CONCLUSIONS

To conclude, we have successfully grown single crystals of a melilite-type ferrimagnet $Eu_2MnSi_2O_7$. The magnetization measurement reveals the easy-plane type magnetic anisotropy where the magnetic moments lie on the tetragonal basal plane. We observe an MSHG signal which scales with the square of the magnetization below the magnetic ordering temperature. The interference of the MSHG with the crystallographic contribution of the same order results in nearly perfect magnetic switching of the SHG intensity where the signal intensity changes by more than 7000%. Such gigantic modulation of nonlinear optical activity may be useful for magnetic sensors or magneto-optical switching devices.

ACKNOWLEDGMENTS

This work was supported by JSPS KAKENHI Grants No. JP18K14154, No. JP20H01867, and No. JP22H01185 as well as by the National Science and Technology Council and National Center for Theoretical Sciences in Taiwan.

[1] Y. Tokura and N. Nagaosa, Nat. Commun. **9**, 3740 (2018).
[2] T. Arima, J. Phys.: Condens. Matter **20**, 434211 (2008).
[3] S. Toyoda, N. Abe, S. Kimura, Y. H. Matsuda, T. Nomura, A. Ikeda, S. Takeyama, and T. Arima, Phys. Rev. Lett. **115**, 267207 (2015).
[4] K. Park, M. O. Yokosuk, M. Goryca, J. J. Yang, S. A. Crooker, S. W. Cheong, K. Haule, D. Vanderbilt, H. S. Kim, and J. L. Musfeldt, npj Quantum Mater. **7**, 38 (2022).
[5] K. Kimura, Y. Otake, and T. Kimura, Nat. Commun. **13**, 697 (2022).

[6] G. L. J. A. Rikken, C. Strohm, and P. Wyder, Phys. Rev. Lett. **89**, 133005 (2002).
[7] I. Kézsmárki, D. Szaller, S. Bordács, V. Kocsis, Y. Tokunaga, Y. Taguchi, H. Murakawa, Y. Tokura, H. Engelkamp, T. Rõõm, and U. Nagel, Nat. Commun. **5**, 3203 (2014).
[8] I. Kézsmárki, N. Kida, H. Murakawa, S. Bordács, Y. Onose, and Y. Tokura, Phys. Rev. Lett. **106**, 057403 (2011).
[9] R. V. Pisarev, I. Sänger, G. A. Petrakovskii, and M. Fiebig, Phys. Rev. Lett. **93**, 037204 (2004).
[10] Y. Ogawa, Y. Kaneko, J. P. He, X. Z. Yu, T. Arima, and Y. Tokura, Phys. Rev. Lett. **92**, 047401 (2004).
[11] M. Matsubara, A. Schmehl, J. Mannhart, D. G. Schlom, and M. Fiebig, Phys. Rev. B **81**, 214447 (2010).
[12] J. Mund, D. R. Yakovlev, A. N. Poddubny, R. M. Dubrovin, M. Bayer, and R. V. Pisarev, Phys. Rev. B **103**, L180410 (2021).
[13] Y. Ogawa, H. Yamada, T. Ogasawara, T. Arima, H. Okamoto, M. Kawasaki, and Y. Tokura, Phys. Rev. Lett. **90**, 217403 (2003).
[14] S. I. Ohkoshi, S. Takano, K. Imoto, M. Yoshikiyo, A. Namai, and H. Tokoro, Nat. Photonics **8**, 65 (2014).
[15] R. P. Pan, H. D. Wei, and Y. R. Shen, Phys. Rev. B **39**, 1229 (1989).
[16] V. V. Pavlov, R. V. Pisarev, A. Kirilyuk, and T. Rasing, Phys. Rev. Lett. **78**, 2004 (1997).
[17] C. Train, T. Nuida, R. Gheorghe, M. Gruselle, and S. I. Ohkoshi, J. Am. Chem. Soc. **131**, 18571 (2009).
[18] S. Toyoda, M. Fiebig, T. H. Arima, Y. Tokura, and N. Ogawa, Sci. Adv. **7**, eabe2793 (2021).
[19] H. Yamada, Y. Ogawa, Y. Ishii, H. Sato, M. Kawasaki, H. Akoh, and Y. Tokura, Science **305**, 646 (2004).
[20] V. V. Pavlov, R. V. Pisarev, M. Fiebig, and D. Fröhlich, Phys. Solid State **45**, 662 (2003).
[21] H. Murakawa, Y. Onose, S. Miyahara, N. Furukawa, and Y. Tokura, Phys. Rev. Lett. **105**, 137202 (2010).
[22] H. Murakawa, Y. Onose, S. Miyahara, N. Furukawa, and Y. Tokura, Phys. Rev. B **85**, 174106 (2012).
[23] H. T. Yi, Y. J. Choi, S. Lee, and S. W. Cheong, Appl. Phys. Lett. **92**, 212904 (2008).
[24] G. A. Petrakovski, L. N. Bezmaternykh, I. A. Gudim, O. A. Bayukov, A. M. Vorotynov, A. F. Bovina, R. Szymczak, M. Baran, and C. Ritter, Phys. Solid State **48**, 1906 (2006).
[25] T. Endo, Y. Doi, M. Wakeshima, and Y. Hinatsu, Inorg. Chem. **49**, 10809 (2010).
[26] A. Zheludev, S. Maslov, G. Shirane, Y. Sasago, N. Koide, and K. Uchinokura, Phys. Rev. Lett. **78**, 4857 (1997).
[27] See Supplemental Material at http://link.aps.org/supplemental/10.1103/PhysRevMaterials.7.024403 for the temperature and magnetic-field dependence of the MSHG signal for (010)-oriented sample, first-principles calculation details, and optical absorption spectrum of $Eu_2MnSi_2O_7$, which includes Refs. [28–38].
[28] J. P. Perdew, K. Burke, and M. Ernzerhof, Phys. Rev. Lett. **77**, 3865 (1996).
[29] S. L. Dudarev, G. A. Botton, S. Y. Savrasov, C. J. Humphreys, and A. P. Sutton, Phys. Rev. B **57**, 1505 (1998).
[30] P. E. Blochl, Phys. Rev. B **50**, 17953 (1994).
[31] G. Kresse and J. Hafner, Phys. Rev. B **47**, 558 (1993).
[32] G. Kresse and J. Furthmuller, Phys. Rev. B **54**, 11169 (1996).
[33] O. Jepson and O. K. Anderson, Solid State Commun. **9**, 1763 (1971).
[34] C. Aversa and J. E. Sipe, Phys. Rev. B **52**, 14636 (1995).
[35] V. K. Gudelli and G.-Y. Guo, Chin. J. Phys. **68**, 896 (2020).
[36] H. Chen, M. Ye, N. Zou, B.-L. Gu, Y. Xu, and W. Duan, Phys. Rev. B **105**, 075123 (2022).
[37] G.-Y. Guo and J. C. Lin, Phys. Rev. B **72**, 075416 (2005).
[38] N. Marzari, A. A. Mostofi, J. R. Yates, I. Souza, and D. Vanderbilt, Rev. Mod. Phys. **84**, 1419 (2012).